RESEARCH ARTICLE

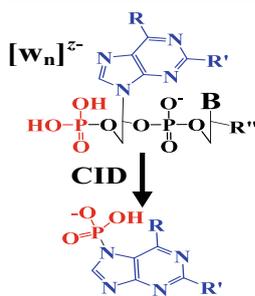# DNA Oligonucleotide Fragment Ion Rearrangements Upon Collision-Induced Dissociation

Brett Harper,[1] Elizabeth K. Neumann,[2] Touradj Solouki[2]

[1]Institute of Biomedical Studies, Baylor University, Waco, TX 76798, USA
[2]Department of Chemistry and Biochemistry, Baylor University, Waco, TX 76798, USA

**Abstract.** Collision-induced dissociation (CID) of *m/z*-isolated w type fragment ions and an intact 5′ phosphorylated DNA oligonucleotide generated rearranged product ions. Of the 21 studied w ions of various nucleotide sequences, fragment ion sizes, and charge states, 18 (~86%) generated rearranged product ions upon CID in a Synapt G2-S HDMS (Waters Corporation, Manchester, England, UK) ion mobility-mass spectrometer. Mass spectrometry (MS), ion mobility spectrometry (IMS), and theoretical modeling data suggest that purine bases can attack the free 5′ phosphate group in w type ions and 5′ phosphorylated DNA to generate sequence permuted [phosphopurine]⁻ fragment ions. We propose and discuss a potential mechanism for generation of rearranged [phosphopurine]⁻ and complementary y-B type product ions.

**Keywords:** Collision-induced dissociation (CID), Ion mobility spectrometry (IMS), Mass spectrometry (MS), Oligonucleotide fragmentation, Rearrangement, w Fragment

## Introduction

The emergence of commercially available electrospray ionization (ESI) sources and high resolving power mass spectrometers has allowed for routine sequencing of oligonucleotides via mass spectrometry (MS) based techniques [1]. Similar to MS sequencing of peptides and proteins [2], to sequence oligonucleotides, precursor molecular ions are generally first isolated and then fragmented using gas-phase dissociation techniques (e.g., CID [3, 4], infrared multiphoton dissociation (IRMPD) [5, 6], electron capture dissociation (ECD) [5], etc.). The resulting product fragment ion mass spectra are then analyzed and interpreted to determine the original nucleotide sequences [7–11].

A potential drawback of oligonucleotide sequencing by tandem MS (MSⁿ) techniques is the data analysis challenges associated with generation of complex mass spectra composed of fragment ions from the 3′ and 5′ ends, internal fragments (generated from sequential fragmentation), and base losses [7].

*Correspondence to:* Touradj Solouki; *e-mail:* Touradj_Solouki@baylor.edu

Although CID of oligonucleotides predominately generates a-B and w type fragment ions (nomenclature of McLuckey et al. [3]), generation of unidentifiable product ions and alternative fragmentation pathways (in CID and other fragmentation techniques) have also been reported [12–15]. For example, Juhasz et al. reported generation of six unusual/unidentifiable high intensity product ion peaks from the DNA oligonucleotide, CAC ACG CCA GT [12]; these authors purported that the presence of unidentifiable fragment ions may make MS based de novo sequencing of some oligonucleotides impractical [12]. Likewise, Nyakas et al. recently described an unusual fragmentation pathway involving loss of internal [PO₃]⁻ through formation of a cyclic intermediate in CID of highly charged DNA oligonucleotides [15].

Because of their potential impact on "top-down" proteomics [16, 17] and high throughput biomolecule sequencing, amino acid "sequence-scrambling" and ion rearrangements in the gas phase have drawn much attention [18–20]. Sequence-scrambling in peptides and proteins are believed to occur through macrocyclization and subsequent reopening at internal amide bonds to generate product ions with rearranged amino acid sequences [21]. Though the impact of rearrangements on sequence coverage of peptides in amino acid sequencing is uncertain [22, 23], positive identification of permuted fragment ions and mechanistic understandings of their generation could

help improve sequencing algorithms. Despite the number of investigations focused on rearrangement pathways of peptide ions, there has been a paucity of examples addressing unusual fragmentation of oligonucleotide ions.

We hypothesized that similar to CID of peptide fragment ions [18–21], CID of DNA fragment ions could also result in generation of secondary fragment ions with rearranged atomic structures (relative to precursor ion structures). For this study, we chose to focus on CID of w type fragment ions for two reasons: (1) w type ions (along with a-B type ions) are the most commonly observed fragment ions in CID of DNA ions [3] and are, thus, often used for sequencing [7–11]; (2) w type ions retain all of the bases in the precursor ion series (unlike a-B type ions, which lack nucleobases at various positions [3]).

In this manuscript, we report the first experimental evidence for generation of rearranged fragment ions during CID of isolated w type oligonucleotide ions and 5′ phosphorylated DNA. We performed CID on 21 $[w_n]^{z-}$ (where n = 1–8 and z = 1–3) fragment ions from three different DNA oligonucleotides. Of the 21 studied w type fragments, ~86% showed evidence for subsequence rearrangement upon CID. We also compared our results to CID of a 5′ phosphorylated DNA oligonucleotide, which showed similar results.

# Experimental

## Sample Preparation

Imidazole and angiotensin II antipeptide (amino acid sequence: EGVYVHPV; used as a lock mass) were purchased from Sigma-Aldrich (St. Louis, MO, USA). Optima grade methanol and water were purchased from Fisher Scientific (Pittsburgh, PA, USA). All DNA oligonucleotides (Oligo-1 [ATG CGT CCG GCG TAG A], Oligo-2 [p-GTA GA; where "p" denotes a 5′ phosphorylation], Oligo-3 [TCG AGG TCG ACG GTA TC], and Oligo-4 [AGA GTT TGA TCC TGG CTC AG]) were purchased from Integrated DNA Technologies (Coralville, IA, USA). Oligo-1, 3, and 4 were chosen based on their small sizes (i.e., ≤20 nucleotides), presence of all four normally occurring DNA bases (i.e., A, G, T, and C) in their sequences, and occurrence of different, nonrepeating nucleotide sequences. Oligo-2 was custom-synthesized to be homologous with the sequence of the $[w_5]^{z-}$ [where "z" denotes the charge state(s)] fragment ions from Oligo-1. Micromolar concentrations of oligonucleotides were prepared in a spray solvent containing 1.0 mM imidazole in a 1:1 mixture of water:methanol. All chemicals and analytes were used "as is" without any additional purification or modification.

## Instrumentation

*Ion Mobility-Mass Spectrometry*   IM-MS experiments were performed using a Synapt G2-S HDMS ion mobility-mass spectrometer (Waters Corporation, Manchester, England, UK) operated in negative-ion mode ESI. The time-of-flight (TOF) mass analyzer was operated either in high resolution mode (i.e., "W" mode for IM experiments in Figure 3 and to distinguish between potential isobaric species) or sensitivity mode (i.e., "V" mode for all other experiments to detect low abundance ions). The experimental scan time for data acquisition was set at 1 s.

Sample flow rate was set at 5 µL/min (Figure 3) or 1.5 µL/min (Figures 1 and 2, and Tables 1 and 2) using a Harvard Pump 11 Plus dual syringe pump (Harvard Apparatus, Holliston, MA, USA). Ion source temperature was set at 100°C and its voltage was set at –3.0 kV for all IM-MS experiments. The software-defined sampling cone voltage was set at –150.0 V (Figures 1a and 2, and Tables 1 and 2), –35.0 V (Figure 1b), or –120.0 V (Figure 3). The ion source offset voltage was set at –35.0 V (Figure 1b) or –150.0 V (all other Figures/Tables). Please note that source conditions were "softer" for Figure 1b to prevent in-source fragmentation. Ion isolation parameters (i.e., quadrupole rf/DC) were optimized to isolate the isotopic distribution of the ions of interest.

Post-IM/CID [24] was performed by setting a 40.0 to 50.0 V (Figure 1 and Tables 1 and 2) or 20.0 V (Figure 2) potential difference between the IM and transfer cells. Pre-IM/CID (Figure 3) was performed by setting a 30.0 V potential difference between the trap and helium cells. IM cell wave height and velocity were set at 40.0 V and 750 m/s, respectively, and nitrogen gas ($N_2$) pressure in the IM cell was ~$3.5 \times 10^{-3}$ bar ($N_2$ flow rate of 90.0 mL/min). Helium gas (used for collisional cooling prior to IM [25]) pressure in the helium cell was ~1.4 bar (helium gas flow rate of 180 mL/min). Argon gas pressures in the trap and transfer cells were both kept at ~$2.4 \times 10^{-5}$ bar (argon gas flow rate of 2.0 mL/min). All gas pressures are reported as direct instrument readouts and have not been corrected for geometry [26, 27] or sensitivity factors [28].

*Ion Trap Mass Spectrometry*   A linear trap quadrupole (LTQ) Orbitrap MS (Thermo Fisher Scientific, Waltham, MA, USA) operated in negative-ion mode ESI was used to collect the $MS^n$ data in Figure 4 and Supplementary Figure S2 in Supporting Information. Mass resolving power ($M/\Delta M_{50\%}$) of the Orbitrap MS was set to the highest resolving power for the instrument (i.e., ~30,000 at m/z 400). Sample flow rate was set to 20 µL/min. The sheath and auxiliary gas ($N_2$) flow rates were set to 60 and 5 AU, respectively. The source, capillary, and tube lens voltages were optimized to –5.0 kV, –42.0 V, and –133.7 V, respectively. The metal capillary temperature was set to 275°C. The entire isotopic distribution of the ions of interest were isolated and fragmented in the LTQ at normalized collision energies [29] of 30% (Figure 4) or 20% (Supplementary Figure S2). Wideband excitation [29] was turned off to minimize reactivation of fragment ions. Helium gas was used as the collision gas for CID (partial pressure of ~$1.3 \times 10^{-8}$ bar). Owing to low abundance of y-B type ions from Oligo-2, sufficiently high sample concentration (100 µM) was used to collect the data displayed in Figure 4. Singly- and doubly-deprotonated angiotensin II antipeptide ions (m/z 897 and

448, respectively) were used as lock masses for all LTQ Orbitrap experiments.

## Data Analysis

IM-MS data were analyzed using MassLynx software (ver. 4.1) (Waters Corporation, Manchester, England, UK). To obtain signal-to-noise ratios of >3 for all ions of interest, acquired IM-MS spectra were averaged for 5 min (Figure 1 and Tables 1 and 2), 10 min (Figure 2), or 20 min (Figure 3). IM profiles displayed in Figure 3 correspond to the centroid $m/z \pm 0.02$ Th, extracted from the associated mass spectra.

LTQ Orbitrap MS data were analyzed using Xcalibur (ver. 2.2) (Thermo Fisher Scientific, Waltham, MA, USA). The data in Figure 4 and Supplementary Figure S2 correspond to the average of 50 and 150 scans, respectively, which provided signal-to-noise ratios of >3 for all ions of interest. Mass measurement error (MME) for all ions identified using the LTQ Orbitrap were ≤ 2 ppm.

Fragment ions corresponding to "typical" losses were identified using Mongo Oligo Mass Calculator (ver. 2.06) [30]. All fragment ion assignments were based on the nomenclature of McLuckey et al. [3]. Unless otherwise indicated (viz., figure caption for Figure 1a), fragment ion identities were assigned with respect to the original oligonucleotide's sequence.

## Theoretical Calculations

Theoretical calculations were performed using density functional theory (DFT) at B3LYP/6-31G(d) level of theory and basis set [31] with Gaussian 09 suite of programs (Gaussian Inc., Wallingford, CT, USA) [32]. Thermochemical data are reported as thermally corrected changes in Gibbs free energies at 298 K ($\Delta G_{298}$) and are expressed in kcal/mol.

# Results and Discussion

## Fragment Ion Rearrangements in CID of w Type and Intact 5′ Phosphorylated Oligonucleotide Ions

Figure 1a shows the MS$^n$ CID mass spectrum of $m/z$-isolated $[w_5]^{2-}$ ($m/z$ 802) generated from in-source CID of Oligo-1 in a Synapt G2-S HDMS system. Under our experimental conditions, CID of $[w_5]^{2-}$ generated two unusual product ions at $m/z$ 214 and 230 (denoted in bold-red font, Figure 1a) which could not be assigned to a known fragment ion type using conventional nomenclature or fragmentation mechanisms. Calculated low MMEs for the assigned peaks suggested that chemical compositions of these observed ions at $m/z$ 214 and 230 might correspond to metaphosphate ($[PO_3]^-$) ion [15] plus adenine (i.e., [phosphoadenine]$^-$; ~5.84 ppm) and $[PO_3]^-$ plus guanine (i.e., [phosphoguanine]$^-$; ~5.96 ppm), respectively. Fragment ion assignments of [phosphoadenine]$^-$ ($m/z$ 214) and [phosphoguanine]$^-$ ($m/z$ 230) are further supported by the presence of complementary fragment ions $[y_5 - A]^-$ ($m/z$

1390) and $[y_5 - G]^-$ ($m/z$ 1374) in the CID mass spectrum of $[w_5]^{2-}$ (denoted in bold-red font, Figure 1a).

Numerous investigations of peptide ion scrambling indicate that fragment ions (e.g., b-type ions; Roepstorff and Fohlman's nomenclature [33]) generated during CID of peptide ions are themselves rearranged, and that the evidence of such rearrangements (i.e., "scrambled" fragment ions) can be observed upon subsequent fragmentation [27, 34–39]. If a similar "scrambling" trend holds true for generation of [phosphoadenine]$^-$ ($m/z$ 214) and [phosphoguanine]$^-$ ($m/z$ 230), the precursor w type ion (i.e., $[w_5]^{2-}$) may also be structurally rearranged. To test this hypothesis, and to determine if [phosphopurines]$^-$ (i.e., [phosphoadenine]$^-$ and [phosphoguanine]$^-$) could be produced from CID of intact 5′ phosphorylated DNA, we performed an analogous experiment to that presented in Figure 1a on a 5′ phosphorylated oligonucleotide (i.e., Oligo-2) with the same sequence as the last five nucleotides of Oligo-1 (i.e., p-GTA GA). Figure 1b shows the CID mass spectrum of $m/z$-isolated doubly charged Oligo-2 (i.e., [Oligo-2 – 2H]$^{2-}$ at $m/z$ 802).

The CID mass spectrum of [Oligo-2 – 2H]$^{2-}$ (Figure 1b) is essentially identical to the CID mass spectrum of $m/z$ isolated $[w_5]^{2-}$ fragment ion ($m/z$ 802) generated from in-source CID of Oligo-1 (Figure 1a). It should be noted that both [phosphopurines]$^-$ and complementary y-B fragment ions (denoted in bold-red font, Figure 1a and b) were present in both mass spectra, and with comparable fragment ion relative abundances. Although we cannot eliminate the possibility that Oligo-2 cyclizes/rearranges prior to fragmentation (e.g., during the ionization process), results in Figure 1b show that the observed [phosphopurines]$^-$ can be generated from the originally linear structures. Therefore, it is likely that isolated $[w_5]^{2-}$ (Figure 1a) is also a linear structure (i.e., not cyclized). This is especially important for sequencing efforts as rearranged w type ions could undermine the validity of MS-based DNA sequencing. Furthermore, results from Figure 1b indicate that in addition to w type ions, 5′ phosphorylated oligonucleotides can also generate [phosphopurines]$^-$.

To confirm the presumed identities of [phosphoadenine]$^-$ ($m/z$ 214) and [phosphoguanine]$^-$ ($m/z$ 230), MS$^n$ experiments (Figure 2a and b, respectively) were carried out. As expected, CID of [phosphoadenine]$^-$ species generated a high intensity peak at $m/z$ 79 (corresponding to $[PO_3]^-$) and a low intensity peak for [adenine]$^-$ (at $m/z$ value of 134) (Figure 2a). Similarly, CID of [phosphoguanine]$^-$ ($m/z$ 230) also generated a high intensity peak for $[PO_3]^-$ (at $m/z$ 79) and a low intensity peak for [guanine]$^-$ (at $m/z$ value of 150) (Figure 2b). Data from the MS/MS mass spectra show that the relative abundance of [adenine]$^-$ with respect to $[PO_3]^-$ (i.e., [adenine]$^-$/$[PO_3]^-$ in Figure 2a) is higher than that observed for [guanine]$^-$ (i.e., [guanine]$^-$/ $[PO_3]^-$ in Figure 2b). These results are in agreement with findings by Pan et al., who demonstrated that [adenine]$^-$ is more stable than [guanine]$^-$ and, therefore, more likely to be generated during the CID of deprotonated DNA oligonucleotides [40].

Experimental results in Figure 2 are further supported by predictions from theoretical calculations (Scheme 1), which suggest that formation of $[PO_3]^-$ ($m/z$ 79) and a corresponding
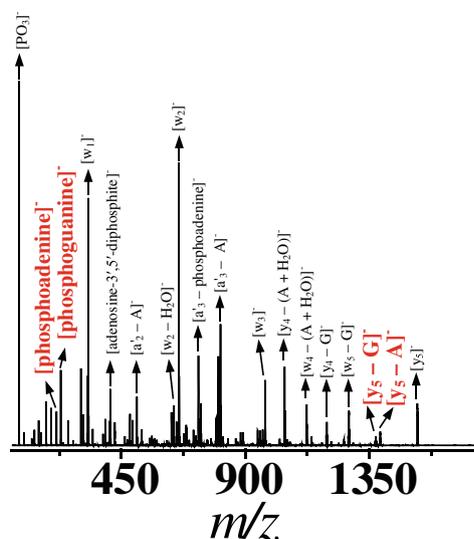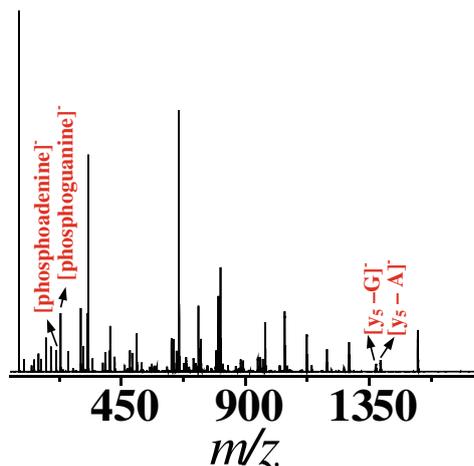
**(a)** **ESI Oligo-1 → In-source CID → Isolate [w$_5$]$^{2-}$ → Post-IM/CID → Mass Spectrum**



**(b)** **ESI Oligo-2 → Isolate [Oligo-2 – 2H]$^{2-}$ → Post-IM/CID → Mass Spectrum**



**Figure 1.** CID mass spectra of $m/z$-isolated **(a)** [w$_5$]$^{2-}$ ($m/z$ 802) generated from in-source CID of Oligo-1, and **(b)** doubly charged intact Oligo-2 ([Oligo-2 – 2H]$^{2-}$ at $m/z$ 802). Sequence for both ions is p-GTA GA. Rearranged [phosphopurine]$^-$ and complementary y-B type ions (see discussion in main text) are denoted in bold-red font. Peaks labeled with a prime sign (e.g., [a′$_3$ – A]$^-$ at $m/z$ 810) denote a-B type fragment ions, which were generated from a precursor w type ion

neutral base (i.e., adenine or guanine; Scheme 1, pathways 1 and 3, respectively) are lower energy dissociation pathways for [phosphopurines]$^-$ than for the formation of neutral HPO$_3$ and purine ions (i.e., [adenine]$^-$ ($m/z$ 134) or [guanine]$^-$ ($m/z$ 150); Scheme 1, pathways 2 and 4, respectively). For example, the $\Delta G_{298}$ for generation of neutral HPO$_3$ and [adenine]$^-$ from [phosphoadenine]$^-$ (Scheme 1, pathway 2) is 48.07 kcal/mol, whereas the $\Delta G_{298}$ for generation of [PO$_3$]$^-$ and neutral adenine (Scheme 1, pathway 1) is 22.73 kcal/mol (i.e., $\Delta G' = -25.33$ kcal/mol, where "$\Delta G'$" denotes the difference in $\Delta G_{298}$ between the two pathways). Similar results were observed for [phosphoguanine]$^-$ pathways (Scheme 1, pathways 3 and 4; $\Delta G' = -17.49$ kcal/mol), suggesting that generation of [PO$_3$]$^-$ is a lower energy pathway than formation of [guanine]$^-$. Although the general trends between theoretical (Scheme 1) and

experimental (Figure 2) evidences are in agreement, an in-depth study of reaction kinetics (e.g., activation barrier(s) to formation and depletion of reactants/products, charge affinities, stability of transition species, etc.) would be necessary to draw concrete conclusions. While useful, these types of calculations are outside the scope of the current manuscript, but may be worth exploring in future studies.

The DNA oligonucleotides used in this study do not contain any non-natural bases or modified groups. Therefore, presence of peaks corresponding to [phosphoadenine]$^-$ ($m/z$ 214) and [phosphoguanine]$^-$ ($m/z$ 230), in Figures 1 and 2, indicates the existence of reaction channels involving intramolecular rearrangements. In other words, based on the high mass measurement accuracy (or MME < 6.00 ppm), observed peaks at $m/z$ 214.0137 and 230.0060 (compared with theoretical $m/z$ values of
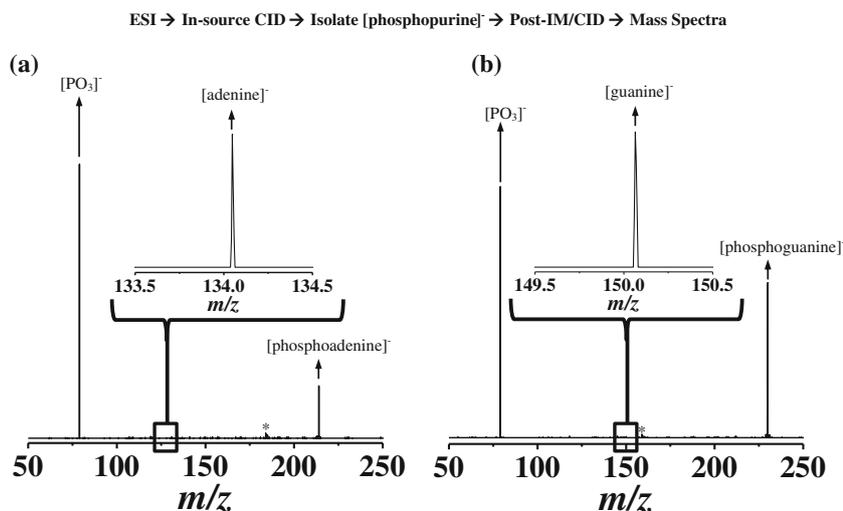
ESI → In-source CID → Isolate [phosphopurine]⁻ → Post-IM/CID → Mass Spectra



**Figure 2.** Post-IM/CID mass spectra of **(a)** [phosphoadenine]⁻ ($m/z$ 214), and **(b)** [phosphoguanine]⁻ ($m/z$ 230). Insets for $m/z$ ranges 133.5 to 134.5 and 149.5 to 150.5 are shown shown at 150× and 250x y-scale expansion, respectively. Peaks marked with an asterisk (*) denote background noise

214.0125 and 230.0074, respectively) can be assigned to negatively charged [phosphoadenine]⁻ and [phosphoguanine]⁻ (i.e., exclusively as rearranged fragment ions). Presence of such rearranged phosphopurine fragment ions may be more prevalent than previously believed. For example, Schulten et al., observed analogous "phosphorous acid + nucleobase" ions in a positive-ion mode pyrolysis field desorption (Py-FD)-MS study [41]. In their discussion, Schulten et al. confer that they could not determine how "phosphorous acid + nucleobase" ions were generated, but

assumed that it was due to pyrolysis of starting materials [41]. In the present study, however, negative ions were generated via CID of ESI-generated species; hence, no pyrolysis products were formed.

Similar to CID of $[w_5]^{2-}$ (Figure 1), CID of $[w_n]^{z-}$ (where n = 2–4, 6, and 7; $z$ = 1 or 2) also generated [phosphoadenine]⁻ ($m/z$ 214) and [phosphoguanine]⁻ ($m/z$ 230) species (Table 1). Of the studied w type ions from Oligo-1, only $[w_1]^-$ ($m/z$ 330) did not generate a [phosphopurine]⁻ (Table 1). Although
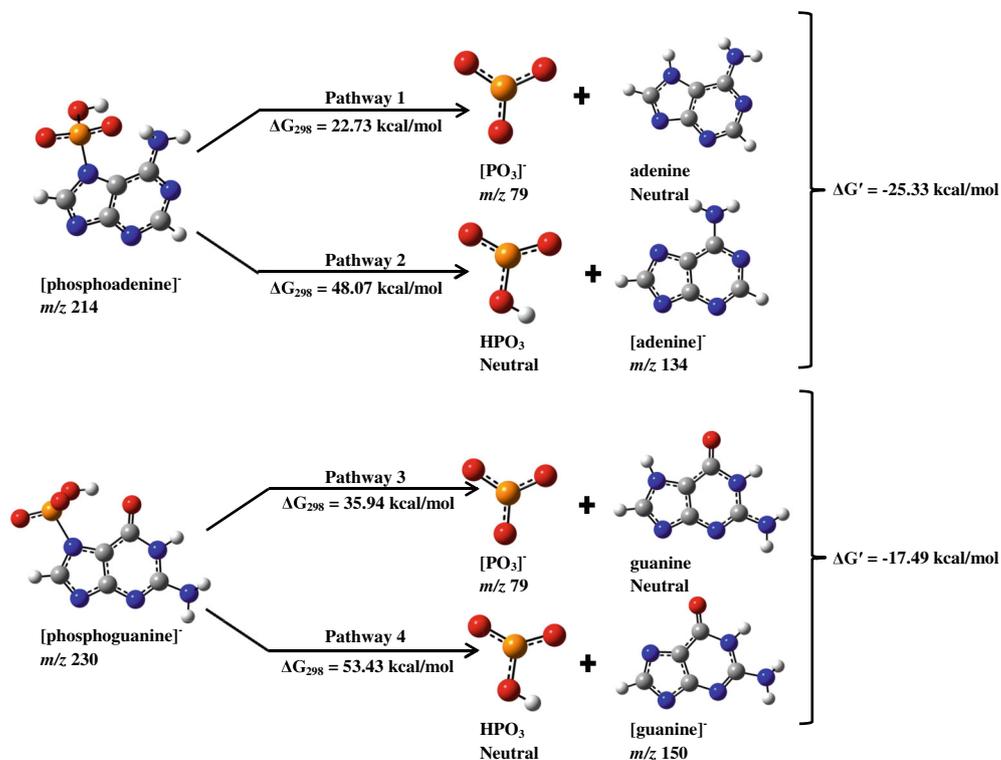


**Scheme 1.** Theoretical pathways for dissociation of [phosphoadenine]⁻ (pathways 1 and 2) and [phosphoguanine]⁻ (pathways 3 and 4)

**Table 1.** Summary of Precursor w Ion Sizes, Charge States, and Presence or Absence of [phosphoadenine]⁻ ($m/z$ 214) and [phosphoguanine]⁻ ($m/z$ 230) Generated from Oligo-1

| $w_n$ | z | $m/z$ 214 | $m/z$ 230 |
|---|---|---|---|
| Oligo-1: ATG CGT CCG GCG TAG A | | | |
| 1 | 1- | ✗ | – |
| 2 | 1- | ✓ | ✓ |
| 3 | 1- | ✓ | ✓ |
| 4 | 2- | ✓ | ✓ |
| 5 | 2- | ✓ | ✓ |
| 6 | 2- | ✓ | ✓ |
| 7 | 2- | ✓ | ✓ |

"–" Denotes that [phosphoguanine]⁻ generation was not possible because of lack of guanine in the precursor w type fragment ion sequence

structural rigidity of the smaller $[w_1]^-$ (compared with large w type ions) may restrict rearrangement reactions, the absence of $m/z$ 214 ([phosphoadenine]⁻) in the CID mass spectrum of $[w_1]^-$ is surprising for two reasons: (1) $[w_1]^-$ contains an adenine in its structure; (2) CID of $[w_2]^-$ from Oligo-1 (Table 1, row 4) generates [phosphoadenine]⁻ ($m/z$ 214) *and* [phosphoguanine]⁻ ($m/z$ 230), suggesting that losses are possible from both positions. These unusual results may be explained by the existence of other lower energy dissociation pathways for $[w_1]^-$, such as those resulting from charge localization [40, 42–44]. For example, Pan et al. demonstrated that deprotonating a phosphate group enhances the proton affinity and, therefore, cleavage of the neighboring nucleobase [40]. In the cases of $[w_n]^{2-}$ fragment ions where n ≥ 2, the negative charge(s) can be distributed to multiple sites in the oligonucleotide, thereby decreasing the chance of a negative charge being at the 5′ terminal phosphate group. The $[w_1]^-$ fragment ion, however, has only one phosphate group that can be deprotonated. Thus, according to previously reported findings [40, 42], charge localization to the 5′ terminal phosphate group could increase the proton affinity of the neighboring adenine and direct fragmentation through loss of adenine, rather than generation of [phosphoadenine]⁻.

To study the conformation(s) of rearranged [phosphopurines]⁻ and check the possibility of the phosphorus-containing group being attached to multiple purine ring positions (i.e., structural isomers), we acquired ion mobility spectra of [phosphoadenine]⁻ ($m/z$ 214) and [phosphoguanine]⁻ ($m/z$ 230) (Figure 3). Presence of multiple structural isomers for each [phosphopurine]⁻ would be indicated by presence of multiple IM arrival time (AT) peaks. IM profiles for [phosphoadenine]⁻ ($m/z$ 214) and [phosphoguanine]⁻ ($m/z$ 230) (Figure 3) each showed single IM peaks, suggesting the presence of a single structure (type) for each ion population. However, it is possible for [phosphopurines]⁻ to have multiple isomers or structures that require higher mobility resolving powers for their successful separation. Hence, under our current experimental conditions, the IM-MS results (Figure 3) suggest that the phosphorus-containing group is attached to purine bases at only one position.

In addition to experiments in the Synapt G2-S HDMS system (i.e., Figures 1, 2, and 3), rearranged [phospho-

**ESI → In-source CID → Isolate [w₅]²⁻ → Pre-IM/CID → IM Spectra**
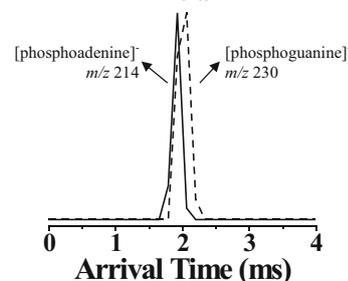


**Figure 3.** IM profiles for [phosphoadenine]⁻ ($m/z$ 214; solid line) and [phosphoguanine]⁻ ($m/z$ 230; dashed line) generated from pre-IM CID of $[w_5]^{2-}$ ($m/z$ 802) from Oligo-1

purines]⁻ were also observed in the CID mass spectra of $[w_5]^{2-}$ from Oligo-1 in a triple quadrupole MS system (Supplementary Figure S1) and [Oligo-2 – 2H]²⁻ in an LTQ Orbitrap MS (Supplementary Figure S2). Results from these three different mass spectrometer types suggest that the [phosphopurine]⁻ fragment ion rearrangement pathway can be accessed in different MS system types and collisional activation regimes. For example, the CID results in Figures 1, 2, and 3 and Supplementary Figure S1 were collected on instruments where collision energy was applied through a voltage potential difference between two electrodes [25, 45]. In this type of nonselective collision regime, product fragment ions continue to undergo collisional activation and fragmentation. Conversely, in the LTQ Orbitrap (Supplementary Figure S2), precursor ions were selectively (i.e., on-resonance) excited and fragmented in the LTQ, which can greatly reduce reactivation (and further fragmentation) of the product fragment ions [29, 46]. Moreover, LTQ Orbitrap results further support the conclusion that the $[y_5 – G]^-$ ($m/z$ 1374) and $[y_5 – A]^-$ ($m/z$ 1390) ions in Figure 1 and Supplementary Figure S2 are complementary fragments to [phosphoguanine]⁻ and [phosphoadenine]⁻, respectively. In other words, these ions might be generated from a common fragmentation pathway (i.e., $[w_5]^{2-} \rightarrow [y_5 – B]^-$) rather than from independent losses (e.g., $[w_5]^{2-} \rightarrow [y_5]^- \rightarrow [y_5 – B]^-$).

To further investigate the fragmentation mechanism for complementary y-B type ions, we performed MSⁿ experiments in the LTQ Orbitrap. Figure 4a and b show the MS³ CID mass spectra of $[y_5 – G]^-$ ($m/z$ 1374) and $[y_5 – A]^-$ ($m/z$ 1390), respectively, generated from Oligo-2 (i.e., isolate [Oligo-2 – 2H]²⁻ ($m/z$ 802) → CID → isolate $[y_5 – G$ or $A]^-$ ($m/z$ 1374 or $m/z$ 1390) → CID to yield the mass spectra in Figure 4). Observed fragments, generated from CID of the ions at $m/z$ 1374 (Figure 4a) and $m/z$ 1390 (Figure 4b), support the fragment ion assignments for $[y_5 – G]^-$ and $[y_5 – A]^-$. Furthermore, none of the product fragment ions generated from CID of isolated $[y_5 – G]^-$ or $[y_5 – A]^-$ precursors suggest the presence of atomic rearrangements or sequence-scrambling, further supporting the conclusion that macrocyclization may not be involved in product ion formation.
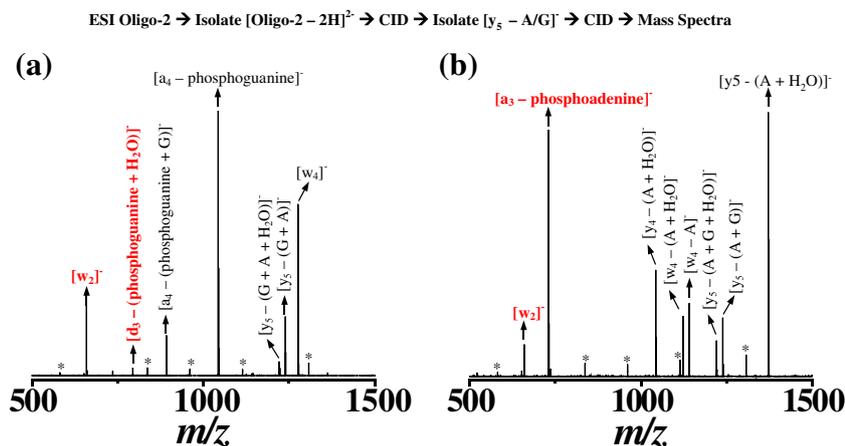
ESI Oligo-2 → Isolate [Oligo-2 – 2H]²⁻ → CID → Isolate [y₅ – A/G]⁻ → CID → Mass Spectra



**Figure 4.** CID mass spectra of $m/z$-isolated **(a)** [y – G]⁻ ($m/z$ 1374), and **(b)** [y – A]⁻ ($m/z$ 1390) generated from Oligo-2 (p-GTA GA) at 30% normalized collision energy. Fragment ions labeled in bold-red font denote peaks that can be used to determine positions of base losses. Peaks marked with an asterisk (*) denote electronic noise

Beyond confirming the fragment ion identities, the CID mass spectra in Figure 4 can also be probed to determine sites of guanine and adenine losses. For example, CID of $[y_5 - G]^-$ (Figure 4a) generated two ions (denoted in bold-red font) at $m/z$ 659 and 794, which correspond to $[w_2]^-$ and $[d_3 - (\text{phosphoguanine} + H_2O)]^-$, respectively. Presence of the $[w_2]^-$ ($m/z$ 659) fragment ion suggests that the guanine at position four (from the 5′ end) is not lost. Moreover, presence of the ion at $m/z$ 794 (i.e., $[d_3 - (\text{phosphoguanine} + H_2O)]^-$) suggests that the guanine at the first position (from the 5′ end) is lost. These two pieces of information together can be used to conclude that at least a portion of the [phosphoguanine]⁻ ions observed at $m/z$ 230 in Figures 1, 2, and 3, and Supplemental Figures S1 and S2, are generated from losses of the guanines at the first positions from the 5′ ends of $[w_5]^{2-}$ and [Oligo-2 – 2H]²⁻. Although the results in Figure 4a suggest that a guanine is lost from the first position, they do not negate the possibility for the presence of multiple pathways to form a [phosphoguanine]⁻ (i.e., from the guanines at positions one and/or four); in other words, observed ions at $m/z$ 230 could be a mixture of these two [phosphoguanine]⁻ populations. Similar conclusions can be drawn from the CID mass spectra of $[y_5 - A]^-$ ($m/z$ 1390) in Figure 4b. CID of $[y_5 - A]^-$ ($m/z$ 1390) generated two fragment ions (denoted in bold-red font) at $m/z$ 659 (again corresponding to the $[w_2]^-$ ion) and $m/z$ 730, corresponding to $[a_3 - \text{phosphoadenine}]^-$ (Figure 4b). Identities of these two ions suggest that adenine is lost from position three; similarly, this finding alone cannot be used to conclusively establish that adenine is not lost from position five as well.

Our MS$^n$ and IM-MS results suggest that [phosphopurines]⁻ are generated from atomic rearrangement of Oligo-1 (ATG CGT CCG GCG TAG A) w type ions and intact 5′ phosphorylated Oligo-2 (p-GTA GA). In the following section, we provide additional experimental data that confirm the prevalence of [phosphopurine]⁻ fragment ion formation (i.e., we show that formation of rearranged [phosphopurine]⁻ fragments

are not limited to CID of w type ions from Oligo-1 and intact Oligo-2).

## Fragment Ion Rearrangements in CID of w Type Ions from Additional DNA Oligonucleotides

Based on the results from CID of $[w_n]^{2-}$ (where n = 1–7; z = 1 or 2) from Oligo-1 (Table 1), we hypothesized that CID of w type ions from other oligonucleotides should also generate [phosphoadenine]⁻ ($m/z$ 214) and/or [phosphoguanine]⁻ ($m/z$ 230), assuming there is an adenine and/or guanine in the nucleotide sequence. To test this hypothesis, we performed additional CID experiments on 14 $[w_n]^{2-}$ (where n = 1–8; z = 1–3) ions (validation set) generated from two DNA oligonucleotides: Oligo-3 (TCG AGG TCG ACG GTA TC) and Oligo-4 (AGA GTT TGA TCC TGG CTC AG). These CID results are summarized in Table 2. Please note that no $[w_3]^{2-}$

**Table 2.** Summary of Precursor w Ion Sizes, Charge States, and Presence or Absence of [phosphoadenine]⁻ ($m/z$ 214) and [phosphoguanine]⁻ ($m/z$ 230) Generated from Validation Set

| $w_n$ | z | $m/z$ 214 | $m/z$ 230 |
|---|---|---|---|
| Oligo-3: TCG AGG TCG ACG GTA TC | | | |
| 1 | 1- | – | – |
| 2 | 1- | – | – |
| 3 | 1- | ✓ | – |
| 4 | 2- | ✓ | – |
| 5 | 2- | ✓ | ✓ |
| 6 | 2- | ✓ | ✓ |
| 7 | 2- | ✓ | ✓ |
| 8 | 3- | ✓ | ✓ |
| Oligo-4: AGA GTT TGA TCC TGG CTC AG | | | |
| 1 | 1- | – | ✗ |
| 2 | 1- | ✓ | ✓ |
| 4 | 2- | ✓ | ✓ |
| 5 | 2- | ✓ | ✓ |
| 6 | 2- | ✓ | ✓ |
| 7 | 2- | ✓ | ✓ |

"–" Denotes that [phosphopurine]⁻ generation was not possible because of lack of guanine and/or adenine in the precursor w type fragment ion sequence

ions were generated from in-source CID of Oligo-4 and are thus absent in Table 2.

Results from CID of $[w_n]^{z-}$ (where n = 1–8; z = 1–3) ions from Oligo-3 and Oligo-4 confirm our hypothesis that [phosphopurine]$^-$ ions can be generated from oligonucleotides with different sequences. Based on our experimental results, the precursor ions' charge state (where z = 1–3) did not have any noticeable effect on generation of [phosphopurine]$^-$ ions; however, potential effects of the precursor ion's charge state on [phosphopurine]$^-$ generation when z > 3 (which were not tested here) should not be negated. The precursor ions' sizes did have some influence on [phosphopurine]$^-$ generation. Notably, [phosphopurine]$^-$ ions were only formed from precursor $[w_n]^{z-}$ ions when n ≥ 2 (i.e., w type ions containing more than one nucleotide in their sequences), which agree with results from CID of $[w_1]^-$ from Oligo-1 (Table 1).

In total, we performed tandem MS experiments on 21 w type ions (Tables 1 and 2) and no [phosphopyrimidine]$^-$ product ions were observed in any of the MS$^n$ experiments. Preferential generation of [phosphopurine]$^-$ over [phosphopyrimidine]$^-$ suggests that the bicyclic nitrogenous ring structure of purines might be essential for formation of intermediate and/or final product ions and their stability. Based on a valuable reviewer comment, we also checked the mass spectra for possibilities of purine interactions with phosphate groups at internal positions, which would be indicated by presence of y + B type ions; however, under our experimental conditions, these types of ions were not observed. It is possible that steric hindrance from the next sequential deoxyribose group may prevent this type of rearrangement (i.e., the rearrangement must involve a terminal phosphate group). These results confirm our IM and MS$^n$ data and are in agreement with the theoretical evidence and allow elucidation of a potential mechanism for formation of [phosphopurine]$^-$ ions.

Scheme 2 shows a proposed mechanism for generation of [phosphopurine]$^-$ (i.e., [phosphoadenine]$^-$ (m/z 214) and

[phosphoguanine]$^-$ (m/z 230)) and complementary y-B type ions (i.e., $[y_n - A]^{(z-1)-}$ and $[y_n - G]^{(z-1)-}$) from CID of m/z-isolated $[w_n]^{z-}$ ions. Please note that the purine base depicted in Scheme 2 could either be guanine or adenine and that nucleobases denoted by a capital "B" could be any nucleobase (i.e., A, G, C, or T). For succinctness, the oligonucleotide structure in Scheme 2 is abbreviated to three nucleotides and we only show the interaction of a purine at nucleobase position two (from the 5′ terminus) with the 5′ phosphate group, although purines at other positions can also follow the same mechanism. The first step in the formation of [phosphopurines]$^-$ may proceed via a mechanism similar to one recently proposed by Stucki et al. in a study of homo-DNA oligonucleotides [47]. First, a lone pair of electrons from the ether oxygen (of the deoxyribose sugar) initiates cleavage of the purine base from the sugar backbone and subsequent nucleophilic attack of the 5′ phosphate group to form a phosphoamide tetrahedral transition species (Scheme 2, Step 1). Next, the phosphoamide tetrahedral transition species can rearrange to generate [phosphopurine]$^-$ (m/z 214 and 230) (Scheme 2, Step 2), which may be structurally similar to phosphoimidazole [48–50]. Finally, neutralization of the oxonium ion may be achieved by β-elimination of a proton from the deoxyribose sugar by one of the adjacent phosphate groups (dashed arrows in Scheme 2, Step 3), moving the pi electrons back to the valence shell of the ether oxygen and generating complementary y-B type ions (Scheme 2, Step 3).

## Conclusion

Our experimental and theoretical results indicate that CID of m/z-isolated 5′ phosphorylated DNA oligonucleotide ions can generate rearranged product ions. Furthermore, CID results suggest that unlike peptide ion rearrangements [18–20],
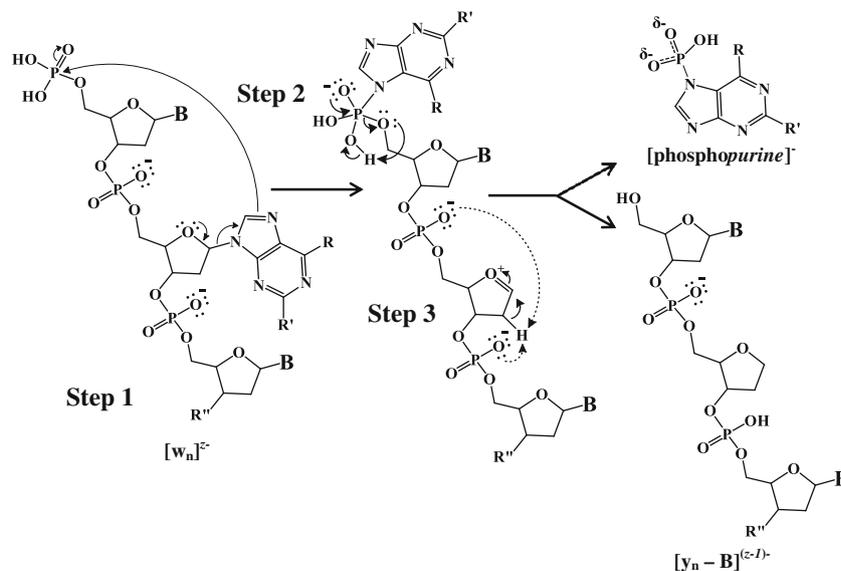


**Scheme 2.** Proposed mechanism for generation of rearranged [phosphopurine]$^-$ and y-B type ions

oligonucleotide ions do not necessarily need to go through a macrocyclic intermediate to generate [phosphopurines]⁻. The proposed mechanism for generation of [phosphopurine]⁻ ions also indicates a previously undefined pathway for formation of y-B type fragment ions.

The predictability of [phosphopurine]⁻ formation may be leveraged as an additional probe to determine if an unknown DNA sequence (or fragment ion) contains a 5′ phosphate group, assuming its sequence contains an adenine and/or guanine nucleobase. Moreover, the predictable nature of [phosphopurine]⁻ formation and incorporation of these fragmentation pathways into existing nucleotide sequencing software/algorithms could improve data analysis.

Although the presence of the two reported [phosphopurine]⁻ ions may be inconsequential to sequence analysis of oligonucleotides, their presence in the CID mass spectra of oligonucleotide ions opens up the possibility that other, more consequential, rearrangements or fragmentation pathways may also exist. The current report gives a small snapshot of how oligonucleotide ions rearrange upon CID. Additional systematic studies are necessary to determine the full extent of oligonucleotide ion rearrangements (e.g., from CID of intact, a, b, c, d, w, x, y, and z type ions [3]) and their effects on sequencing efforts.

## Acknowledgments

## References

1. Meng, Z., Simmons-Willis, T.A., Limbach, P.A.: The use of mass spectrometry in genomics. Biomol. Eng. **21**, 1–13 (2004)

2. Sadygov, R.G., Cociorva, D., Yates III, J.R.: Large-scale database searching using tandem mass spectra: looking up the answer in the back of the book. Nat. Methods **1**, 195–202 (2004)

3. McLuckey, S.A., Van Berkel, G.J., Glish, G.L.: Tandem mass spectrometry of small, multiply charged oligonucleotides. J. Am. Soc. Mass Spectrom. **3**, 60–70 (1992)

4. McLuckey, S.A., Habibi-Goudarzi, S.: Decompositions of multiply charged oligonucleotide anions. J. Am. Chem. Soc. **115**, 12085–12095 (1993)

5. Håkansson, K., Hudgins, R., Marshall, A., O'Hair, R.J.: Electron capture dissociation and infrared multiphoton dissociation of oligodeoxynucleotide dications. J. Am. Soc. Mass Spectrom. **14**, 23–41 (2003)

6. Keller, K.M., Brodbelt, J.S.: Collisionally activated dissociation and infrared multiphoton dissociation of oligonucleotides in a quadrupole ion trap. Anal. Biochem. **326**, 200–210 (2004)

7. Castleberry, C.M., Rodicio, L.P., Limbach, P.A.: Electrospray ionization mass spectrometry of oligonucleotides. Current Protocols in Nucleic Acid Chemistry, John Wiley & Sons, Inc. 35, Unit 10.2.1-10.2.19 (2008)

8. Murray, K.K.: DNA sequencing by mass spectrometry. J. Mass Spectrom. **31**, 1203–1215 (1996)

9. Nakayama, H., Akiyama, M., Taoka, M., Yamauchi, Y., Nobe, Y., Ishikawa, H., Takahashi, N., Isobe, T.: Ariadne—a database search engine for identification and chemical analysis of RNA using tandem mass spectrometry data. Nucleic Acids Res. **37**, e47 (2009)

10. Ni, J., Pomerantz, S.C., Rozenski, J., Zhang, Y., McCloskey, J.A.: Interpretation of oligonucleotide mass spectra for determination of sequence using electrospray ionization and tandem mass spectrometry. Anal. Chem. **68**, 1989–1999 (1996)

11. Rozenski, J., McCloskey, J.A.: SOS—a simple interactive program for ab initio oligonucleotide sequencing by mass spectrometry. J. Am. Soc. Mass Spectrom. **13**, 200–203 (2002)

12. Juhasz, P., Roskey, M.T., Smirnov, I.P., Haff, L.A., Vestal, M.L., Martin, S.A.: Applications of delayed extraction matrix-assisted laser desorption ionization time-of-flight mass spectrometry to oligonucleotide analysis. Anal. Chem. **68**, 941–946 (1996)

13. Premstaller, A., Huber, C.G.: Factors determining the performance of triple quadrupole, quadrupole ion trap and sector field mass spectrometer in electrospray ionization mass spectrometry. 2. Suitability for de novo sequencing. Rapid Commun. Mass Spectrom. **15**, 1053–1060 (2001)

14. Yang, J., Mo, J., Adamson, J.T., Håkansson, K.: Characterization of oligodeoxynucleotides by electron detachment dissociation fourier transform ion cyclotron resonance mass spectrometry. Anal. Chem. **77**, 1876–1882 (2005)

15. Nyakas, A., Eberle, R., Stucki, S., Schürch, S.: More than charged base loss—revisiting the fragmentation of highly charged oligonucleotides. J. Am. Soc. Mass Spectrom. **25**, 1155–1166 (2014)

16. Bogdanov, B., Smith, R.D.: Proteomics by FTICR mass spectrometry: top down and bottom up. Mass Spectrom. Rev. **24**, 168–200 (2005)

17. Siuti, N., Kelleher, N.L.: Decoding protein modifications using top-down mass spectrometry. Nat. Methods **4**, 817–821 (2007)

18. Tang, X.J., Thibault, P., Boyd, R.K.: Fragmentation reactions of multiply-protonated peptides and implications for sequencing by tandem mass spectrometry with low-energy collision-induced dissociation. Anal. Chem. **65**, 2824–2834 (1993)

19. Riba Garcia, I., Giles, K., Bateman, R.H., Gaskell, S.J.: Studies of peptide a- and b-type fragment ions using stable isotope labeling and integrated ion mobility/tandem mass spectrometry. J. Am. Soc. Mass Spectrom. **19**, 1781–1787 (2008)

20. Miladi, M., Harper, B., Solouki, T.: Evidence for sequence scrambling in collision-induced dissociation of y-type fragment ions. J. Am. Soc. Mass Spectrom. **24**, 1755–1766 (2013)

21. Tirado, M., Polfer, N.C.: Defying entropy: forming large head-to-tail macrocycles in the gas phase. Angew. Chem. Int. Ed. Engl. **124**, 1–4 (2012)

22. Saminathan, I.S., Wang, X.S., Guo, Y., Krakovska, O., Voisin, S., Hopkinson, A.C., Siu, K.W.: The extent and effects of peptide sequence scrambling via formation of macrocyclic B ions in model proteins. J. Am. Soc. Mass Spectrom. **21**, 2085–2094 (2010)

23. Goloborodko, A.A., Gorshkov, M.V., Good, D.M., Zubarev, R.A.: Sequence scrambling in shotgun proteomics is negligible. J. Am. Soc. Mass Spectrom. **22**, 1121–1124 (2011)

24. Hoaglund-Hyzer, C.S., Li, J., Clemmer, D.E.: Mobility labeling for parallel CID of ion mixtures. Anal. Chem. **72**, 2737–2740 (2000)

25. Giles, K., Williams, J.P., Campuzano, I.: Enhancements in travelling wave ion mobility resolution. Rapid Commun. Mass Spectrom. **25**, 1559–1566 (2011)

26. Solouki, T., Szulejko, J.: Bimolecular and unimolecular contributions to the disparate self-chemical ionizations of α-Pinene and camphene isomers. J. Am. Soc. Mass Spectrom. **18**, 2026–2039 (2007)

27. Zekavat, B., Miladi, M., Al-Fdeilat, A., Somogyi, A., Solouki, T.: Evidence for sequence scrambling and divergent H/D exchange reactions of doubly-charged isobaric b-type fragment ions. J. Am. Soc. Mass Spectrom. **25**, 226–236 (2014)

28. Bartmess, J.E., Georgiadis, R.M.: Empirical methods for determination of ionization gauge relative sensitivities for different gases. Vacuum **33**, 149–153 (1983)

29. Lopez, L.L., Tiller, P.R., Senko, M.W., Schwartz, J.C.: Automated strategies for obtaining standardized collisionally induced dissociation spectra on a benchtop ion trap mass spectrometer. Rapid Commun. Mass Spectrom. **13**, 663–668 (1999)

30. Rozenski, J.: Mongo Oligo Mass Calculator v2.06 Available at: http://mods.rna.albany.edu/masspec/Mongo-Oligo. The RNA Institute, College of Arts and Sciences, State University of New York at Albany (1999)

31. Francl, M.M., Pietro, W.J., Hehre, W.J., Binkley, J.S., Gordon, M.S., DeFrees, D.J., Pople, J.A.: Self-consistent molecular orbital methods. XXIII. A polarization-type basis set for second-row elements. J. Chem. Phys. **77**, 3654–3665 (1982)

32. Frisch, M., Trucks, G., Schlegel, H., Scuseria, G., Robb, M., Cheeseman, J., Scalmani, G., Barone, V., Mennucci, B., Petersson, G., Nakatsuji, H.,Caricato, M., Li, X., Hratchian, H., Izmaylov, A., Bloino, J., Zheng, G., Sonnenberg, J.,Hada, M., Ehara, M., Toyota, K., Fukuda, R., Hasegawa, J., Ishida, M., Nakajima, T., Honda, Y., Kitao, O., Nakai, H., Vreven, T., Montgomery Jr., J., Peralta, J., Ogliaro, F.,Bearpark, M., Heyd, J., Brothers, E., Kudin, K., Staroverov, V., Keith, T., Kobayashi, R., Normand, J., Raghavachari, K., Rendell, A., Burant, J., Iyengar, S., Tomasi, J., Cossi, M., Rega, N., Millam, J., Klene, M., Knox, J., Cross, J., Bakken, V., Adamo, C., Jaramillo, J., Gomperts, R., Stratmann, R., Yazyev, O., Austin, A., Cammi, R., Pomelli, C., Ochterski, J., Martin, R., Morokuma, K., Zakrzewski, V., Voth, G., Salvador, P., Dannenberg, J., Dapprich, S., Daniels, A., Farkas, O., Foresman, J., Ortiz, J., Cioslowski, J., Fox, D.: Gaussian 09, Rev. C. 01. Gaussian. Inc, Wallingford, CT (2010)

33. Roepstorff, P., Fohlman, J.: Proposal for a common nomenclature for sequence ions in mass spectra of peptides. Biomed. Mass Spectrom. **11**, 601 (1984)

34. Zekavat, B., Miladi, M., Becker, C., Munisamy, S., Solouki, T.: Combined use of post-ion mobility/collision-induced dissociation and chemometrics for b fragment ion analysis. J. Am. Soc. Mass Spectrom. **24**, 1355–1365 (2013)

35. Fattahi, A., Zekavat, B., Solouki, T.: H/D Exchange kinetics: experimental evidence for formation of different b fragment ion conformers/isomers during the gas-phase peptide sequencing. J. Am. Soc. Mass Spectrom. **21**, 358–369 (2010)

36. Erlekam, U., Bythell, B.J., Scuderi, D., Van Stipdonk, M., Paizs, B., Maître, P.: Infrared spectroscopy of fragments of protonated peptides: direct evidence for macrocyclic structures of b5 ions. J. Am. Chem. Soc. **131**, 11503–11508 (2009)

37. Riba-Garcia, I., Giles, K., Bateman, R., Gaskell, S.: Evidence for structural variants of a- and b-type peptide fragment ions using combined ion mobility/mass spectrometry. J. Am. Soc. Mass Spectrom. **19**, 609–613 (2008)

38. Polfer, N.C., Bohrer, B.C., Plasencia, M.D., Paizs, B., Clemmer, D.E.: On the dynamics of fragment isomerization in collision-induced dissociation of peptides. J. Phys. Chem. A **112**, 1286–1293 (2008)

39. Bleiholder, C., Osburn, S., Williams, T.D., Suhai, S., Van Stipdonk, M., Harrison, A.G., Paizs, B.: Sequence-scrambling fragmentation pathways of protonated peptides. J. Am. Chem. Soc. **130**, 17774–17789 (2008)

40. Pan, S., Verhoeven, K., Lee, J.K.: Investigation of the initial fragmentation of oligodeoxynucleotides in a quadrupole ion trap: charge level-related base loss. J. Am. Soc. Mass Spectrom. **16**, 1853–1865 (2005)

41. Schulten, H.R., Beckey, H.D., Boerboom, A.J.H., Meuzelaar, H.L.C.: Pyrolysis field desorption mass spectrometry of deoxyribonucleic acid. Anal. Chem. **45**, 2358–2362 (1973)

42. Green-Church, K.B., Limbach, P.A.: Mononucleotide gas-phase proton affinities as determined by the kinetic method. J. Am. Soc. Mass Spectrom. **11**, 24–32 (2000)

43. Bythell, B.J., Knapp-Mohammady, M., Paizs, B., Harrison, A.G.: Effect of the His residue on the cyclization of b ions. J. Am. Soc. Mass Spectrom. **21**, 1352–1363 (2010)

44. Molesworth, S.P., Van Stipdonk, M.J.: Apparent inhibition by arginine of macrocyclic b ion formation from singly charged protonated peptides. J. Am. Soc. Mass Spectrom. **21**, 1322–1328 (2010)

45. Giles, K., Pringle, S.D., Worthington, K.R., Little, D., Wildgoose, J.L., Bateman, R.H.: Applications of a travelling wave-based radio-frequency-only stacked ring ion guide. Rapid Commun. Mass Spectrom. **18**, 2401–2414 (2004)

46. Campbell, J.M., Collings, B.A., Douglas, D.J.: A new linear ion trap time-of-flight system with tandem mass spectrometry capabilities. Rapid Commun. Mass Spectrom. **12**, 1463–1474 (1998)

47. Stucki, S., Désiron, C., Nyakas, A., Marti, S., Leumann, C., Schürch, S.: Gas-phase dissociation of homo-DNA oligonucleotides. J. Am. Soc. Mass Spectrom. **24**, 1997–2006 (2013)

48. Kee, J.-M., Villani, B., Carpenter, L.R., Muir, T.W.: Development of stable phosphohistidine analogues. J. Am. Chem. Soc. **132**, 14327–14329 (2010)

49. Attwood, P.V.: PN bond protein phosphatases. Biochim Biophys Acta, Proteins Proteomics **1834**, 470–478 (2013)

50. Attwood, P., Piggott, M.J., Zu, X.L., Besant, P.G.: Focus on phosphohistidine. Amino Acids **32**, 145–156 (2007)